

Controlling Chaos in El Niño

Douglas G. MacMynowski

Abstract—Many weather and climate phenomena are chaotic in nature; indeed for many people this is the canonical example of a chaotic system. However, because of this, it is at least theoretically possible to have significant influence over these systems with extremely small control inputs. This potential is explored using the Cane-Zebiak 33 000-state model of the El-Niño/Southern Oscillation (ENSO). The model dynamics are nonlinear and chaotic, and the optimal control input can be found through iteration using the adjoint simulation. The performance of this optimal control (which implicitly assumes perfect model and state information) is compared with a simple SISO linear feedback. Significant reductions in ENSO amplitude are (theoretically) possible with very small control inputs, illustrating that it is possible to have significant influence over large-scale climatic phenomena without correspondingly large control effort.

I. INTRODUCTION

The El-Niño/Southern Oscillation (ENSO) is the largest coherent inter-annual signal in the climate, affecting rainfall and temperature patterns across the globe. It arises from coupled atmosphere/ocean physics in the tropical Pacific ocean [1]–[3] with a dominant period of El Niño events (anomalously warm eastern Pacific; see Fig. 3) between two and seven years. The irregular dynamics have been explained either as the result of a stable system driven by stochastic forcing from the rest of the climate system, or an unstable system exhibiting self-sustained chaos [4] and possibly even switching between these two cases depending on the background climatic state.

Lorenz' original observation of chaos was with respect to weather and climate [5], and this remains today as the canonical example of chaos in popular literature. The sensitivity to arbitrarily small perturbations in initial conditions also means that chaotic systems are sensitive to small control inputs. This observation has been made for control of weather generally [6] and hurricane track or strength [7, 8] in particular. An algorithm has also been presented to influence the future evolution of chaotic ENSO dynamics [9], however, the goal was to demonstrate chaos-control techniques for stabilizing an unstable periodic orbit in a complicated system, not to reduce ENSO amplitude. Of course, to take advantage of the sensitivity of chaotic dynamics in a real system would in principle require perfect knowledge of both the dynamics and the state; understanding the trade-off between control effort and knowledge is beyond the scope of this paper.

In exploring control of chaotic dynamics in ENSO, it is not my intent to suggest that we should intentionally interfere

in the climate system and control ENSO, although it may be worth considering that option if climate change leads to significant shifts in ENSO behaviour. There are nonetheless several interesting reasons for exploring control. The primary reason is to use this as a case study to illustrate that chaotic dynamics, ubiquitous in weather and climate systems, can be controlled with extremely small inputs. While not surprising, this can change how we think about the scale of human interaction with the climate system. Additionally, understanding what feedbacks have the potential to substantially alter ENSO can aid in understanding future responses to anthropogenic climate changes.

A simple linear control strategy for ENSO is presented in [10]; results are extended here to consider optimal (non-linear) control that takes into account full knowledge of the chaotic dynamics in order to achieve comparable reduction in ENSO with much smaller control input energy. The mechanism proposed in [10] for influencing ENSO dynamics is to dynamically modulate the absorbed solar insolation in the eastern tropical Pacific. A plausible means for doing so is to influence the cloud albedo by modifying the density of cloud condensation nuclei; this has been suggested for planetary solar radiation management to partially compensate for anthropogenic climate change [11, 12]. If this form of geoengineering is eventually implemented, then the potential to also control ENSO will automatically be available. While this may not be the most energetically efficient way to influence ENSO, the available solar power over the Niño-3 region of the eastern tropical Pacific is roughly a factor of 10^4 larger than the maximum power involved in an El Niño event, and thus even small modulation of solar insolation can have a significant influence on the state trajectory.

The next section describes the dynamics and modeling of ENSO, including relevant energetics (summarized from [10]). The Cane-Zebiak intermediate complexity model [13] is used herein; this model is sufficiently complex to be representative of climate simulations and preclude simple analysis, yet computationally simple enough to use as a numerical experiment. The optimal control is obtained from the adjoint simulation, which is constructed from the forward model using automatic differentiation [14]. Control results using both linear and the nonlinear optimum are presented in Sec. III.

II. MODEL

A brief discussion of ENSO physics is relevant to understanding the dynamics; see e.g. [2] for more details.

The mean tropical Pacific climate state is driven by westward trade winds, which leads to a westward surface

D. G. MacMynowski is in the Department of Control and Dynamical Systems, California Institute of Technology, Pasadena, CA 91125. macmardg@cds.caltech.edu

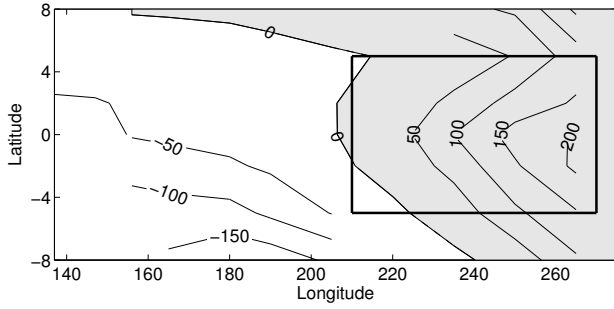


Fig. 1. Mean distribution of available potential energy in tropical Pacific, in kJ/m^2 , computed from TAO data. The Niño-3 region is boxed; shading indicates positive APE. Adapted from [10].

current. Mass conservation implies ocean upwelling in the eastern Pacific; the eastern Pacific is therefore colder, and the thermocline that separates cold deep water from warmer mixed surface water is shallower than in the west. The longitudinal sea surface temperature (SST) gradient reinforces the westward atmospheric winds because warmer air in the western Pacific rises, leading to stronger zonal winds from mass conservation. Bjerknes first noted this positive feedback, which makes the tropical Pacific system less stable, and unstable with the parameters in the model used here. It is the mean thermocline slope that provides the storage of potential energy that drives the unsteady behaviour [15] (changes in kinetic energy are much smaller).

For a shallow water model (an upper layer with density $(1 - \delta)\rho_0$ over a deep layer of density ρ_0), the energy per unit surface area is

$$APE = \frac{1}{2} \delta \rho_0 g |h| h \quad (1)$$

where h is the depth displacement relative to its mean (over the basin and over time), g is gravity (the reduced gravity is $g_{\text{red}} = \delta g$). Using this approximation, the mean distribution of APE is shown in Fig 1, computed from the TAO array of ocean bouys. The variation in energy over the Niño-3 region ($\pm 5^\circ$ latitude, 150° W to 90° W) over the course of the 1998 El Niño event is of order 10^{18}J , and the maximum power flow into or out of this region is roughly 100 GW, and this thus provides an upper bound on the work required to modify ENSO dynamics through ocean forcing.

This APE is sustained by 0.2 to 0.4 TW of mean atmospheric wind power [16], corresponding to roughly 0.01% of the solar radiation absorbed over the Niño-3 region. That is, only a fraction of the wind energy is converted into potential energy that can influence ENSO, and only a fraction of the solar energy is converted into wind energy. While this is thus a less efficient mechanism for influencing ENSO, it is easier to envision modulating insolation by modulating cloud albedo than it is to envision directly modulating ocean currents. In the model described below, heating perturbations are applied directly, and the corresponding fraction of solar power estimated from

$$Q = \frac{C_p \rho H \Delta T}{Q_{\text{sol}}} \quad (2)$$

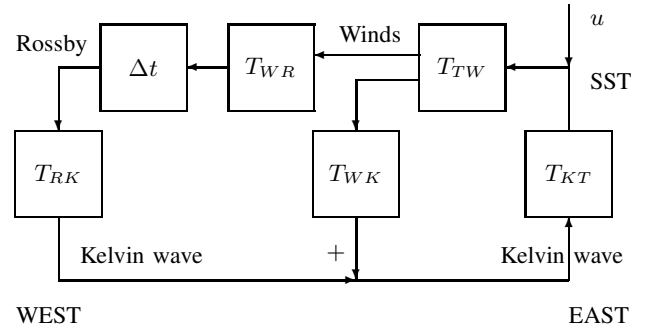


Fig. 2. Schematic of ENSO delayed-oscillator dynamics. The righthand feedback loop represents the eastern-Pacific physics where SST anomalies lead to changes in wind which excite Kelvin waves. The lefthand feedback loop represents the delayed effect including excitation of Rossby waves, and reflection off the western boundary, to create a Kelvin wave. Time delays and external disturbances are not explicitly shown; the control input u influences the SST directly.

for heat capacity C_p and surface mixed layer depth of H (the mean over the eastern half of the Niño-3 region is 28 m); Q is normalized by the mean surface solar insolation, roughly $Q_{\text{sol}} = 250 \text{ W/m}^2$.

The basic physics of the ENSO cycle can be described conceptually as a delayed oscillator [17], illustrated schematically in Fig. 2, although of course the real dynamics are much more complicated. A perturbation in eastern-Pacific SST, for example, leads to a perturbation in mid-Pacific winds. The wind stress excites ocean Kelvin and Rossby waves. The former propagate eastward, changing the depth of the eastern-Pacific thermocline, the upwelling temperature, and reinforce the original perturbation. The Rossby waves travel westward more slowly, reflect off the western boundary as an eastward-propagating Kelvin wave, which eventually counteracts the original anomaly. This simple description leads to an oscillator, as there will still be non-zero wave amplitudes in the western Pacific by the time the eastern Pacific returns to equilibrium. The average periodicity in the real ocean is between 2 and 7 years; an El Niño event corresponds to anomalously warm eastern Pacific SST (e.g. Fig. 3), while the opposite La Niña phase corresponds to anomalously cold eastern Pacific conditions.

The model used here is from Zebiak and Cane [13], which computes anomalies from a specified monthly-mean climatological background state. The horizontal equations of motion for a single layer atmosphere and single layer ocean are discretized over the tropical Pacific, with the ocean thermocline depth also varying. The vertical currents and winds are much smaller, but critical to the dynamics, and the relevant effects are parameterized. This includes the upwelling effect on ocean SST, and heat release due to condensation from uprising air in the atmosphere, with vertical velocity inferred from convergence or divergence in the horizontal fields. This leads to a computationally efficient 33 000 state nonlinear time-varying model that captures the essential dynamic features of ENSO. See [13] for details on the equations; the dominant nonlinear effect is in the ocean upwelling parameterization, and the model is time-periodic

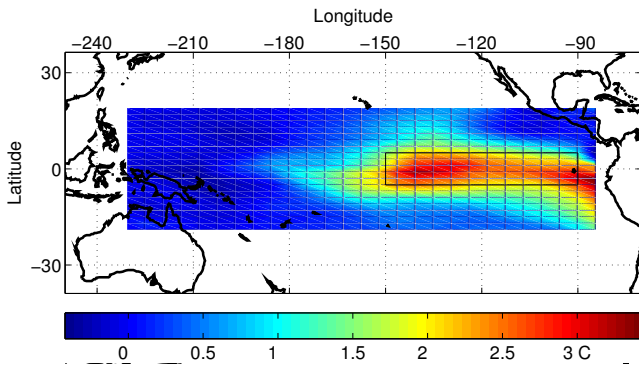


Fig. 3. SST anomaly predicted by model at the peak of an El Niño event (at ~ 19 yrs in the uncontrolled time-history in Fig. 6(a)). The Niño-3 region is shown boxed. For control, solar insolation is dynamically varied over the eastern half of the Niño-3 region.

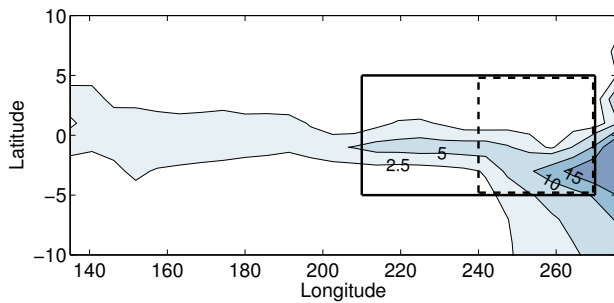


Fig. 4. Optimal distribution of forcing; change in Niño-3 index for change in solar radiation over one grid cell ($2^\circ \times 5.625^\circ$) for excitation at 4-year period. The Niño-3 region is shown boxed, the forcing region used is shown with dashed lines. Adapted from [10].

due to the background seasonal cycle. Using the original parameters in [13] the dominant eigenvalue corresponding to the ENSO oscillation is unstable [18], and an irregular cycle is obtained as a result of chaotic dynamics [4].

The tangent linear adjoint simulation is obtained from the forward simulation code using automatic differentiation, using Adifor 2.1 [14].

III. CONTROL

The most effective spatial distribution of forcing is computed in [10] for small amplitude perturbations about the zero-anomaly equilibrium state; the distribution of effectiveness is reproduced here as Fig. 4. The most effective place to modulate solar insolation in order to influence the long-term evolution of ENSO is the eastern Pacific; roughly the eastern-half of the Niño-3 region (this is partly because of the strong influence of SST changes on winds, and partly because the shallower mixed-layer depth means it takes smaller perturbations to the absorbed solar radiation to obtain the same change in SST).

An adjoint simulation could also be used to refine this spatial sensitivity information taking advantage of the full nonlinear model and computing the optimal sensitivity pattern for a given initial condition and corresponding state trajectory. However, averaging the sensitivity over many different initial conditions is likely to yield a similar answer to

computing the sensitivity for the average (i.e. zero anomaly) initial condition (this is obviously not rigorously true). Also note that the optimal place to force the system for maximum long-term benefit is not necessarily the same location where perturbations have the most significant short-term influence on ENSO. The latter have also been computed using adjoint simulations [19], and correspond to wind perturbations in the central Pacific.

Linear single-input single-output feedback of the Niño-3 index can be used [10]; with u_k as the heating input at time-step k over the eastern tropical Pacific (as in Fig. 4) and y_k as the Niño-3 index, then $u_k = -Ky_k$ is sufficient to stabilize the unstable system. In steady-state, the amplitude of the control is thus non-zero only if there are non-zero disturbances to the system. Figs. 5 and 6 include this strategy; the former shows the effect for increasing feedback gain K . The approach in [10] also included a (nonlinear) adaptive feedforward component to improve the cancellation of incoming Kelvin-wave disturbances, however this had minimal impact on the trade-off between short-term control authority and ENSO amplitude.

However, it may take significant time for the system to reach steady-state, and while the control effort even for the linear SISO control approach is plausible (of order 1% modulation of the incoming solar radiation), it is valuable to understand how much smaller the forcing amplitude could be if complete model information and state information were available. Understanding the trade-off between these two limiting information cases, what state information is most useful, and how to robustly take advantage of some minimal model information without reverting to the higher control effort simple solution would also be valuable.

Given a forward dynamic simulation

$$x_{k+1} = f(x_k, u_k, k) \quad (3)$$

and a performance metric

$$J = \sum_{k=1}^N h(x_k, u_k) \quad (4)$$

then the adjoint code produces the gradient

$$g = \frac{\partial J}{\partial u} \quad (5)$$

If u_k is scalar, then the dimension of the gradient is the number of time-steps N in the simulation (the look-ahead time for the nonlinear optimization). The control time history u_k , $k = 1, \dots, N$ that minimizes J is obtained by

- (i) computing the trajectory x_k evolving from a specified initial condition and initial guess for u_k , $k = 1, \dots, N$,
- (ii) computing the gradient g about this trajectory,
- (iii) conducting a line-search along the gradient direction to minimize the cost J , and
- (iv) iterating this procedure until convergence.

The algorithm is prone to converging to local minima, and the control time history from the SISO feedback strategy is used here as an initial guess. Because the forward simulations

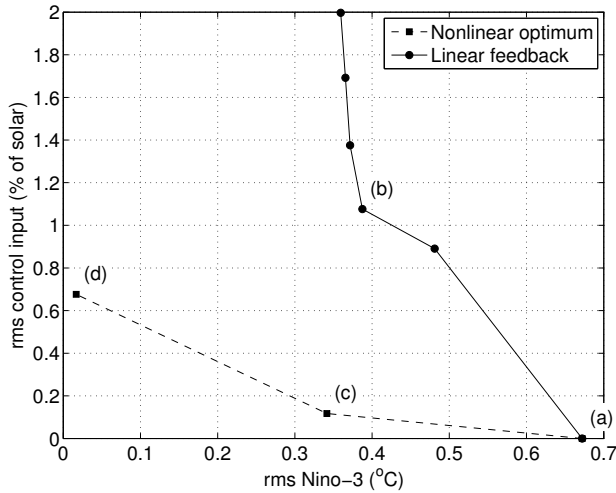


Fig. 5. Performance vs. control effort, comparing SISO linear feedback with the optimal nonlinear control, for a 25-yr simulation, with no disturbances.

are of order N times faster than the gradient calculation, step (iii) is computationally cheap compared to step (ii). The resulting control time history depends on the initial condition (or observed state at time $k = 0$). A receding-horizon control (RHC) strategy can readily be implemented by applying only the first one (or more) control steps, and repeating the optimization. RHC can be used to add robustness to errors in model or state knowledge.

Here, a quadratic performance metric is used so $h(x_k, u_k) = y_k^2 + \rho u_k^2$ where y_k is the Niño-3 index at time-step k , and ρ can be used to parameterize a trade-off between control effort and reduction in Niño-3 amplitude.

Simulation results are shown in Figs. 5 and 6. Starting from a particular initial condition, control is simulated for a 25-year run using either SISO linear feedback (not requiring any significant or unrealistic model information) or with the optimal nonlinear control input obtained through the adjoint-based optimization. While the linear control does result in eventual convergence to a state of zero anomaly, this can take significant time: at the particular gain illustrated in Fig. 6(b), a quasi-annual-cycle mode is excited that takes several decades to decay. Full state/model information, in contrast, can be used either to achieve comparable reductions in Niño-3 amplitude with almost negligible control effort (case (c), with rms over 25 years of order 0.1% modulation of absorbed solar radiation, with a peak of order 0.5%), or to effectively eliminate the ENSO oscillation altogether with moderate control effort (case (d), with rms of 0.65%, peak of $\sim 3\%$ modulation). Note that the former (higher control weighting) solution results in no extreme-El Niño events over this time interval, in contrast to the two that occur in the uncontrolled time history, yet the control authority required to do so is extremely small.

Of course, in the real world, there are unknown disturbances acting on the system, and the performance of the nonlinear optimum is unlikely to be as good as shown in Figs. 5 and 6; these simulations provide an upper bound on

the performance that could be achieved with full model and state knowledge for this chaotic system.

IV. DISCUSSION

The canonical example of chaotic systems in many people's minds is that of the butterfly influencing the global weather. This sensitivity to perturbations also makes weather and other climate systems amenable to control. This is illustrated here using the El Niño/Southern Oscillation as a case study, and comparing SISO linear feedback to the nonlinear optimal control input. While it is possible to significantly reduce the amplitude of El Niño oscillations with extremely small control input, robustness to model and state uncertainty is clearly an important question; it is not immediately obvious whether the benefit illustrated in Fig. 5 disappears with even small model uncertainty.

Several extensions to the control strategy here are straightforward, with the most relevant being to explore whether the use of an RHC strategy is sufficient to obtain robustness to model uncertainty, state knowledge, or disturbances. Including constraints on the maximum/minimum modulation of solar insolation would be more realistic. While the excitation mechanism is chosen here based on the plausibility of implementation, the exploration of the relative energy requirements of forcing the system at different locations or with different input variables (e.g. extracting energy from ocean currents or atmospheric winds) could be valuable in terms of better understanding of ENSO dynamics.

The key reason for exploring the controllability of ENSO is not to suggest that we should control it, but rather to change our perceptions about the scale of influence we are capable of having on the Earth's climate and weather systems. The climate is no longer something simply imposed upon human endeavours, but intentionally or not, is influenced by them.

V. ACKNOWLEDGMENTS

The adjoint simulation used herein was obtained from the Cane-Zebiak model using Adifor; a collaborative project between the Mathematics and Computer Science Division at Argonne National Laboratory and the Center for Research on Parallel Computation at Rice University.

TAO data used in computing APE are made available by the TAO Project Office of NOAA/PMEL.

REFERENCES

- [1] H. A. Dijkstra, *Nonlinear physical oceanography*. Kluwer Academic Publishers, 2000.
- [2] H. A. Dijkstra and G. Burgers, "Fluid dynamics of El-Niño variability," *Annual Review of Fluid Mechanics*, vol. 34, pp. 531–558, 2002.
- [3] J. D. Neelin, D. S. Battisti, A. C. Hirst, F.-F. Jin, Y. Wakata, T. Yamagata, and S. Zebiak, "ENSO theory," *Special Joint issue of J. Geophys. Res. Atmospheres and J. Geophys. Res. Oceans*, vol. 103, no. C7, pp. 14,261–14,290, 1998.
- [4] E. Tziperman, M. A. Cane, and S. E. Zebiak, "Irregularity and locking to the seasonal cycle in an ENSO prediction model as explained by the quasi-periodicity route to chaos," *J. Atmos. Sci.*, vol. 52, no. 3, pp. 293–306, feb 1 1995.
- [5] E. N. Lorenz, "Deterministic nonperiodic flow," *J. Atmospheric Sciences*, vol. 20, pp. 130–141, 1963.

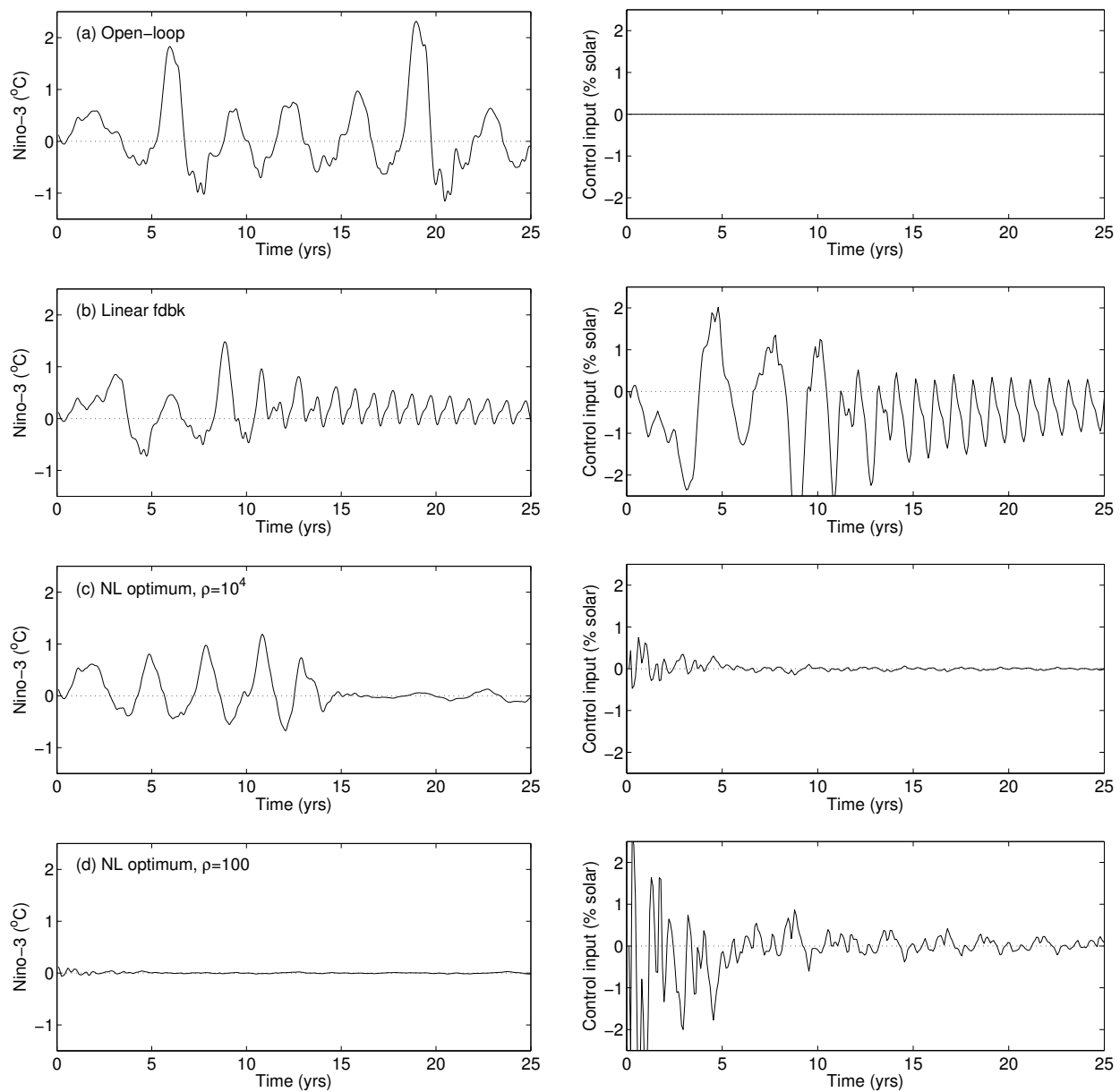


Fig. 6. Time history of Niño-3 index (left) and control input (right) for different control cases. From top to bottom, cases are (a) uncontrolled, (b) linear feedback, (c) nonlinear optimum with high control penalty, and (d) nonlinear optimum with small control penalty, corresponding to cases (a)-(d) in Fig. 5.

- [6] R. N. Hoffman, "Controlling the global weather," *AMS Bulletin*, vol. 83, no. 2, pp. 241–248, Feb. 2002.
- [7] —, "Controlling hurricanes," *Scientific American*, vol. 291, no. 4, pp. 68–75, 2004.
- [8] J. M. Henderson, R. N. Hoffman, S. M. Leidner, T. Nehrkorn, and C. Grassotti, "A 4D-Var study on the potential of weather control and exigent weather forecasting," *Quarterly J. Royal Met. Soc.*, vol. 131, pp. 3037–3051, 2005.
- [9] E. Tziperman, H. Scher, S. E. Zebiak, and M. A. Cane, "Controlling spatiotemporal chaos in a realistic El Niño prediction model," *Physical Review Letters*, vol. 79, no. 6, pp. 1034–1037, aug 11 1997.
- [10] D. G. MacMynowski, "Can we control El Niño?" *Environmental Research Letters*, vol. 4, 2009.
- [11] J. Latham, "Amelioration of global warming by controlled enhancement of the albedo and longevity of low-level maritime clouds," *Atmos. Science Letters*, pp. 52–58, 2002.
- [12] J. Latham, P. Rasch, C.-C. J. Chen, L. Kettles, A. Gadian, A. Gettelman, H. Morrison, K. Bower, and T. Choularton, "Global temperature stabilization via controlled albedo enhancement of low-level maritime clouds," *Philosophical Trans. Royal Society A*, vol. 366, no. 1882, pp. 3969–3987, 2008.
- [13] S. E. Zebiak and M. A. Cane, "A model El Niño-Southern Oscillation," *Mon. Weath. Rev.*, vol. 115, pp. 2262–2278, 1987.
- [14] C. Bischof, A. Carle, G. Corliss, A. Griewank, and P. Hovland, "AD-IFOR: Generating derivative codes from Fortran programs," *Scientific Programming*, vol. 1, no. 1, pp. 11–29, 1992.
- [15] L. Goddard and S. G. Philander, "The energetics of El Niño and La Niña," *J. Climate*, vol. 13, pp. 1496–1516, 2000.
- [16] J. N. Brown and A. V. Fedorov, "Mean energy balance in the tropical Pacific ocean," *J. Marine Research*, vol. 66, no. 1, pp. 1–23, 2008.
- [17] M. J. Suarez and P. S. Schopf, "A delayed action oscillator for ENSO," *J. Atmos. Sci.*, vol. 45, pp. 3283–7, 1988.
- [18] D. G. MacMynowski and E. Tziperman, "Factors affecting ENSO's period," *J. Atmospheric Sciences*, vol. 65, no. 5, pp. 1570–1586, 2008.
- [19] A. M. Moore and R. Kleeman, "The dynamics of error growth and predictability in a coupled model of ENSO," *Q. J. R. Meteorol. Soc.*, vol. 122, pp. 1405–1446, 1996.